Research Square

Preprints are preliminary reports that have not undergone peer review.
They should not be considered conclusive, used to inform clinical practice,
or referenced by the media as validated information.

Concentration- and frequency-associated responses to intramuscular ozone in rat skeletal muscle: functional, mitochondrial, redox, and inflammatory outcomes

Min Liu[1]
Henan University of Chinese Medicine
Yanchen Feng[2]
Heilongjiang University of Chinese Medicine
Jiabin Song[1]
Henan University of Chinese Medicine
Weiqi Li[3]
The Third Affiliated Hospital of Henan University of Chinese Medicine
Tianqi Zhang[1]
Henan University of Chinese Medicine
Youlong Zhou
15938766349@163.com
Henan University of Chinese Medicine

Research Article

Keywords: ozone therapy, skeletal muscle, exposure–response, muscle function, mitochondrial adaptation, oxidative stress, inflammasome, muscle injury

Posted Date: November 13th, 2026

DOI: https://doi.org/10.21203/rs.3.rs-11508832/v1

License: This work is licensed under a Creative Commons Attribution 4.0 International License.
Read Full License

Additional Declarations: No competing interests reported.

Concentration- and frequency-associated responses to intramuscular ozone in rat skeletal muscle: functional, mitochondrial, redox, and inflammatory outcomes

Min Liu[1], Yanchen Feng[2], Jiabin Song[1], Weiqi Li[3], Tianqi Zhang[1] and Youlong Zhou[1]*

[1] The Third Clinical Medical School (College of Acupuncture and Tuina), Henan University of Chinese Medicine, Zhengzhou, Henan 450000, China

[2] School of Basic Medical Sciences, Heilongjiang University of Chinese Medicine, Harbin 150040, China

[3] The Third Affiliated Hospital of Henan University of Chinese Medicine, Henan 450000, China

Correspondence: Youlong Zhou, 15938766349@163.com

Abstract

Background: Intramuscular ozone is used in musculoskeletal practice, but local skeletal-muscle responses to different concentrations and administration frequencies remain incompletely characterized.
Methods: A total of 124 male Sprague–Dawley rats were studied in two stages. The screen included 80 rats assigned to 16 groups and 15 ozone regimens (20–60 μg/mL; 1, 2, or 7 injections/week) for 2 weeks. A separate cohort of 44 rats compared saline control, 30 μg/mL twice weekly (LD-OZ), 60 μg/mL twice weekly (HD-OZ), and 30 μg/mL seven times weekly (HF-OZ) for up to 7 weeks. Endpoints were assessed at prespecified times using endpoint-specific sampling schedules.
Results: In the screen, the quadriceps-to-body-weight ratio averaged 97.1%, 96.8%, and 90.4% of control at 1, 2, and 7 injections/week, respectively; frequency had a significant effect, whereas concentration and interaction did not. LD-OZ was associated with 11% higher grip strength, 71% higher ATP, and 107% higher succinate dehydrogenase activity at week 1. HD-OZ and HF-OZ were associated with 17% and 26% lower grip strength and approximately 40% and 50% lower fibre cross-sectional area. Higher-exposure regimens were also associated with redox changes, inflammatory and NLRP3–GSDMD-related markers, and proteolysis-related changes; collagen area was most clearly increased in HF-OZ. Gross muscle mass did not detect the HD-OZ phenotype.
Conclusions: The findings support a regimen- and endpoint-dependent response pattern compatible with, but not proof of, hormesis-like behaviour. Frequency-matched procedural controls, intermediate regimens, and pathway-directed experiments are needed to clarify specificity and mechanism.

Keywords: ozone therapy; skeletal muscle; exposure–response; muscle function; mitochondrial adaptation; oxidative stress; inflammasome; muscle injury

Background

Medical ozone, generally delivered as an oxygen–ozone (O_2–O_3) mixture, has been evaluated in several musculoskeletal settings, including lumbar disc herniation, knee osteoarthritis, and myofascial pain syndrome [1–4]. Clinical trials and reviews report heterogeneous concentrations and treatment schedules, while systematic preclinical characterization of local skeletal-muscle responses remains limited [5–8]. This gap is relevant to intramuscular and paravertebral procedures, which expose muscle directly or

indirectly to repeated injections. Some patients receiving these interventions may also have age-related reductions in muscle reserve and strength [9–12].

One proposed biological rationale for ozone therapy is that a controlled, transient oxidative challenge may alter redox-sensitive signalling. Ozone reacts rapidly with water and biomolecules, generating hydrogen peroxide (H_2O_2) and lipid ozonation products that may act as secondary messengers [6,13–14]. Under some conditions, redox signalling may engage antioxidant and mitochondrial adaptation; a more intense or more frequent challenge may instead exceed local buffering capacity and be associated with tissue injury [15]. The AMPK–PGC-1α–TFAM axis is involved in mitochondrial regulation, whereas oxidative stress may coincide with inflammasome-related signalling, gasdermin D (GSDMD) cleavage, and proteolysis-related responses [16–17]. These pathways provide a rationale for evaluating multiple endpoints, but their involvement in intramuscular ozone-associated muscle responses requires direct experimental testing.

We therefore used a two-stage rat study to examine how ozone concentration and administration frequency were associated with gross muscle mass and with complementary functional, structural, biochemical, and molecular endpoints [18–19]. The first stage screened 16 regimens for 2 weeks to characterize muscle-mass and serum-biochemistry patterns [20–21]. The second stage compared three ozone regimens with a saline control over 7 weeks, with endpoint-specific sampling at weeks 1, 2, and 7. The study addressed three questions: whether frequency or concentration was more closely associated with gross muscle mass; whether functional, histological, biochemical, or molecular endpoints identified changes not captured by gross muscle mass; and whether the tested regimens showed distinct patterns involving mitochondrial-related responses, redox balance, inflammation, and proteolysis.

Methods

Animals and ethics

A total of 124 specific-pathogen-free male Sprague–Dawley rats (3 months old; approximately 300 ± 20 g) were used: 80 in the initial dose-ranging screen and 44 in the main experiment. Animals were obtained from Jinan Pengyue Laboratory Animal Breeding Co., Ltd. [Animal Production License No. SCXK (Lu) 2022-0006]. They were housed under a 12-h light/12-h dark cycle at 22 ± 2 °C and 55 ± 10% relative humidity, with standard chow and water available ad libitum. Animals were acclimatized before experimentation and were reported to have normal food intake and good general health. The protocol was approved by the Ethics Committee of the Animal Experimental Center of Henan University of Chinese Medicine (approval no. IACUC-202603021). The study was reported in accordance with the ARRIVE 2.0 guidelines.

Ozone generation and intramuscular administration

Rats were anesthetized with 3% sodium pentobarbital (0.2 mL/100 g). Ozone was generated using a medical-grade ozone generator (SYZ-80A, Jinan Sanyan Technology Co., Ltd.), and the ozone concentration was verified immediately before each injection. Because ozone decomposes rapidly, each syringe was prepared and administered within the laboratory-validated time interval. After aseptic disinfection, 20 μL of the ozone preparation was injected into the belly of the right quadriceps femoris muscle using a 100-μL microsyringe. Control animals received an equivalent injection of sterile saline by the same route.

Dose-ranging screen

Eighty rats were allocated to 16 groups (n = 5 per group): one saline-control group and 15 ozone groups covering all combinations of five concentrations (20, 30, 40, 50, and 60 μg/mL) and three administration frequencies (1, 2, or 7 injections per week). Treatment lasted 2 weeks. Body weight was recorded at baseline and at the end of week 2. The quadriceps femoris was then dissected and weighed, and the quadriceps-to-body-weight ratio was calculated. Serum alanine aminotransferase (ALT), aspartate aminotransferase (AST), blood urea nitrogen (BUN), and creatinine (Cr) were measured using commercial colorimetric kits.

Main experiment and treatment regimens

Four regimens were included in the main experiment(Table 1). LD-OZ and HD-OZ shared the same administration frequency and differed in concentration; LD-OZ and HF-OZ used the same concentration and differed in frequency. For descriptive comparison only, nominal weekly exposure was calculated as concentration multiplied by injections per week; this index should not be interpreted as a direct measurement of tissue dose.**Insert Table 1 here**

Table 1. Treatment regimens in the main experiment.

Group	Ozone concentration	Injection frequency	Nominal concentration × frequency index	Experimental contrast
CON	Saline	7×/week	0	Reference
LD-OZ	30 μg/mL	2×/week	60 μg/mL/week	Reference ozone regimen
HD-OZ	60 μg/mL	2×/week	120 μg/mL/week	Concentration doubled vs. LD-OZ
HF-OZ	30 μg/mL	7×/week	210 μg/mL/week	Frequency increased vs. LD-OZ

Note. The index reported as μg/mL/week in the original table is ozone concentration multiplied by injection frequency; it is not an administered ozone mass dose or a direct measure of tissue exposure.

Animals in the main experiment underwent terminal sampling after 1, 2, or 7 weeks. Within each group (n = 11), three animals were sampled at week 1, three at week 2, and five at week 7, giving 12, 12, and

20 animals, respectively, across the four groups at those time points. Endpoint-specific sample sizes were n = 3 per group per time point for immunoblotting, quantitative PCR, and biochemical assays; n = 4 per group for histology and immunofluorescence; n = 5 per group for functional testing; and n = 3 per group for electron microscopy. ATP and succinate dehydrogenase activity were measured in week-1 samples, while selected oxidative-stress and serum-enzyme endpoints were assessed at weeks 1, 2, and 7. Functional testing, histology, and immunofluorescence used overlapping cohorts as described below.

Euthanasia and tissue collection

At the scheduled experimental endpoints (week 2 for the dose-ranging screen and weeks 1, 2, and 7 for the main experiment), rats were administered sodium pentobarbital (100 mg/kg, intraperitoneally) for terminal anaesthesia and euthanasia. Before terminal blood collection, an adequate depth of anaesthesia was confirmed by the absence of the pedal withdrawal reflex in response to a firm toe pinch. Respiratory rate and pattern were also monitored to assess anaesthetic depth. While under deep anaesthesia, blood samples were collected from the abdominal aorta, and exsanguination was performed as a secondary method of euthanasia. Death was confirmed by the sustained absence of spontaneous respiration and heartbeat, assessed by observation of thoracic movements and cardiac auscultation, respectively, for at least 5 min. Following confirmation of death, the quadriceps femoris muscles were excised and processed for subsequent histological, biochemical, and molecular analyses. All procedures were conducted in accordance with the approved institutional animal ethics protocol (IACUC-202603021).

Functional assessments

Grip strength was measured using a calibrated grip-strength meter (HS-MForce-01, Hongshi Scientific Co., Ltd.). Each rat underwent five consecutive trials, and the maximum value was used for analysis. Motor endurance was assessed using an accelerating rotarod. Testing was performed 24 h before scheduled euthanasia by an investigator blinded to group allocation.

Histology, fibre morphometry, and electron microscopy

Quadriceps samples were fixed in 4% paraformaldehyde, embedded in paraffin, sectioned at 3 μm, and stained with hematoxylin and eosin or Masson trichrome. Sections were imaged at 20× (0.794 μm/pixel; field 645 × 476 μm). Collagen deposition was quantified as the fraction of blue-stained area. Fibre cross-sectional area was measured in QuPath v0.7.0 through the paquo Python interface; automated segmentation was reviewed manually, and one field per animal was analysed. For electron microscopy, muscle was fixed in 2.5% glutaraldehyde, post-fixed in osmium tetroxide, embedded, and ultrathin-sectioned. Samples were examined at 80 kV at magnifications of 5000× and 10,000×.

Biochemical assays and cytokines

Muscle 8-hydroxy-2′-deoxyguanosine (8-OHdG), malondialdehyde (MDA), total glutathione (T-GSH), and oxidized glutathione (GSSG) were measured in tissue homogenates and normalized to protein content. Muscle ATP and succinate dehydrogenase activity were measured in week-1 samples. Serum creatine kinase (CK) and lactate dehydrogenase (LDH), together with muscle interleukin-1β (IL-1β) and tumour necrosis factor-α (TNF-α), were measured using commercial kits. Details of tissue homogenization and plate reading are provided in Supplementary Table S1.

Immunoblotting

Quadriceps lysates were separated by SDS-PAGE, transferred to PVDF membranes, and probed for p-AMPK, total AMPK, PGC-1α, TFAM, cytochrome c, NLRP3, ASC, pro-caspase-1, cleaved caspase-1, GSDMD-N, cleaved IL-1β, MuRF1, atrogin-1, and ubiquitin. GAPDH was used as the loading control. Target signals were normalized to GAPDH from the same membrane and then to the mean of the CON group. Three biological replicates were analysed per group.

Quantitative real-time PCR

Total RNA was reverse-transcribed and amplified for Ppargc1a, Tfam, Trim63, and Fbxo32, with Gapdh as the reference gene. Relative quantities were calculated using the $2^{-\Delta\Delta Ct}$ method; statistical testing was performed on ΔCt values. Each sample was run in three technical replicates. Melt curves were reported to be single-peaked, with low variation among technical replicates. Primer sequences are listed in Supplementary Table S3.

Immunofluorescence and TUNEL

Sections were stained for MuRF1 or GSDMD-N with DAPI counterstaining. TUNEL-positive nuclei were expressed as the number of positive nuclei divided by the total number of nuclei, multiplied by 100%. Images were acquired at 20× and quantified in one field per animal by a blinded observer.

Statistical analysis

Data are presented as mean ± SD with individual animal values overlaid where shown. Single-time-point endpoints were analysed using one-way ANOVA followed by Tukey HSD or Dunnett's test against CON. Endpoints measured at weeks 1, 2, and 7 were analysed by two-way ANOVA with group and sampling time as factors, followed by within-time-point comparisons against CON. In the screening phase, concentration and frequency were evaluated by two-way ANOVA. Candidate ordinary least-squares models describing the muscle-mass response were compared using Akaike's information criterion. A broken-stick model was explored descriptively with bootstrap resampling; because its

confidence interval spanned the search grid, no cumulative-exposure breakpoint was treated as established. qPCR analyses used ΔCt values with Benjamini–Hochberg correction within each gene panel. All tests were two-sided, and $p < 0.05$ was considered statistically significant.

Cohort allocation and biological replicates

The study comprised two independent experimental cohorts. The dose-ranging screen included 80 rats in 16 groups (n = 5 per group), with terminal tissue collection after 2 weeks. The main experiment used 44 rats in four groups (CON, LD-OZ, HD-OZ, and HF-OZ; n = 11 per group). Within each group, three rats underwent terminal sampling at week 1, three at week 2, and five at week 7.

At week 7, functional assessments were performed in five rats per group before terminal tissue collection. Of these animals, four per group provided samples for histology and immunofluorescence, and three per group provided samples for transmission electron microscopy. Where technically feasible, different portions of tissue from the same animal were used for additional molecular and biochemical analyses. At weeks 1 and 2, three rats per group provided samples for the scheduled molecular and biochemical analyses.

The individual animal was the experimental unit for each endpoint. Endpoint-specific sample sizes in the Methods and figure legends refer to animals included in each analysis, not separate cohorts for every assay. Some tissue samples from the same animal were used across different assays within a treatment group and sampling time point. Animals terminally sampled at different time points were distinct, and technical replicates were not counted as independent biological replicates.

Results

Injection frequency was more closely associated with gross muscle mass in the screen

Two weeks of ozone exposure did not change body weight or weight gain across the 16 regimens. The quadriceps-to-body-weight ratio varied among groups, and the pattern was more clearly associated with injection frequency than with concentration. When pooled across concentrations, the ratio was 97.1%, 96.8%, and 90.4% of control at one, two, and seven injections per week, respectively. Two-way ANOVA identified a significant frequency effect, whereas the concentration effect and interaction were not significant. Changes in serum ALT, AST, BUN, and Cr were concentrated in the seven-injection-per-week regimens(Fig. 1).

Models containing injection frequency were similar by AIC, whereas concentration alone performed poorly. The exploratory broken-stick analysis did not identify a reproducible breakpoint on the nominal cumulative-exposure scale. Thus, in this screen, gross muscle mass was more sensitive to administration

frequency than to concentration. This finding does not rule out concentration-associated effects on other functional, structural, or molecular endpoints.

Insert Fig. 1 here

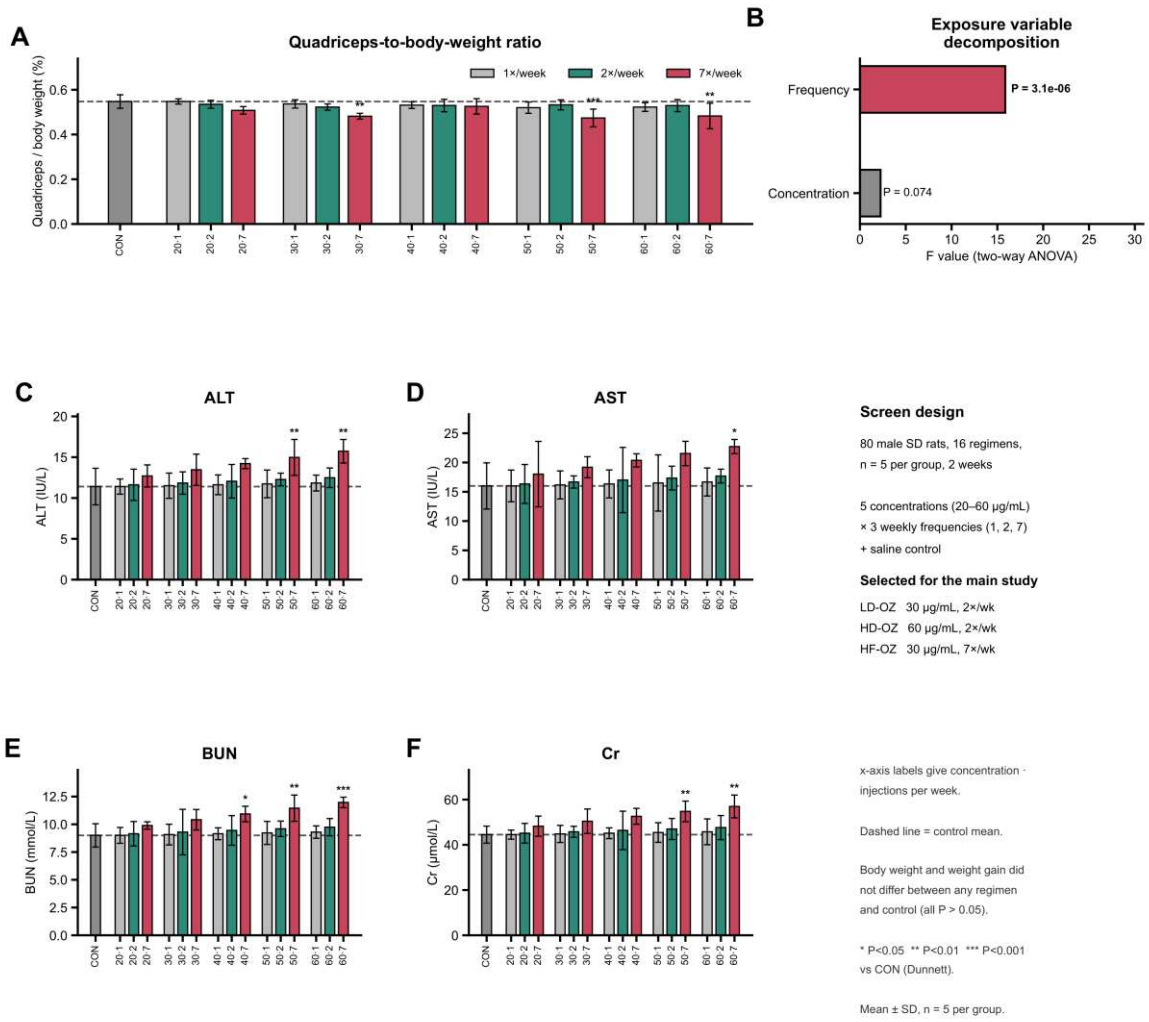


Figure 1. Dose-ranging screen across 16 regimens. (A) Quadriceps-to-body-weight ratio. (B) Two-way ANOVA decomposition of the ratio. (C–F) Serum ALT, AST, BUN, and Cr. Bars show mean ± SD with individual animals overlaid; n = 5 per group. The dashed line indicates the control mean. Statistical symbols indicate comparisons versus CON as defined in the text.

Functional and structural endpoints distinguished the three ozone regimens

In the main experiment, grip strength was 11% higher in LD-OZ than in CON. In contrast, grip strength was 17% lower in HD-OZ and 26% lower in HF-OZ. Rotarod latency was less discriminating, although performance was lower in the higher-exposure groups than in the control group.

Fibre cross-sectional area was not detectably changed in LD-OZ but was approximately 40% lower in HD-OZ and 50% lower in HF-OZ. Collagen area increased most clearly in HF-OZ(Fig.2). The association between fibre area and grip strength was strong when all groups were pooled but weak within individual groups, suggesting that the pooled relationship was driven mainly by separation between

treatment groups. Notably, gross muscle mass remained close to control in HD-OZ in the screening experiment, despite lower grip strength and fibre area in the main experiment.

Insert Fig. 2 here

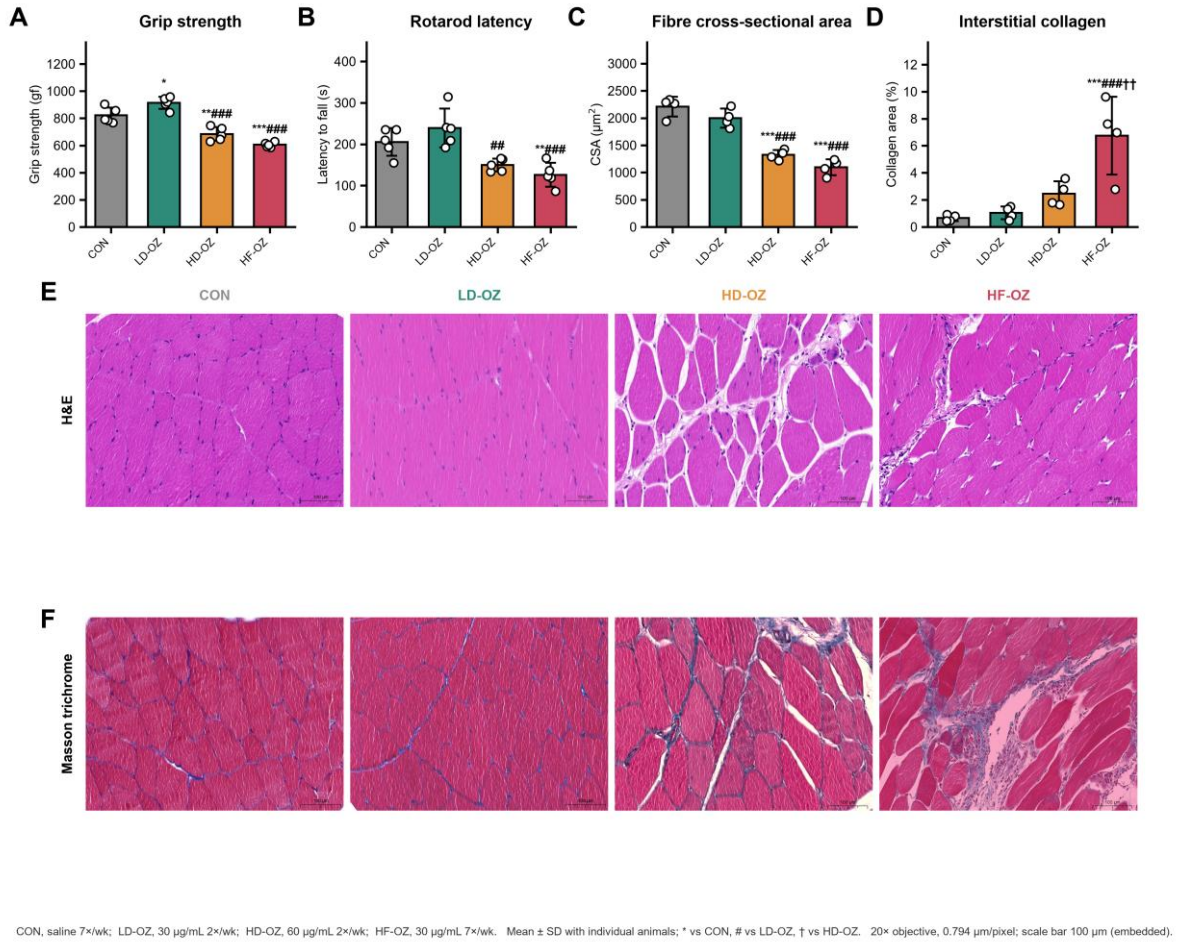


Figure 2. Functional, morphometric, and histological outcomes. (A) Grip strength. (B) Rotarod latency. (C) Fibre cross-sectional area. (D) Interstitial collagen area fraction. (E) Representative hematoxylin and eosin sections. (F) Representative Masson trichrome sections. Data are mean ± SD with individual animals overlaid. n = 5 for functional testing and n = 4 for morphometry and collagen quantification. Scale bars, 100 µm.

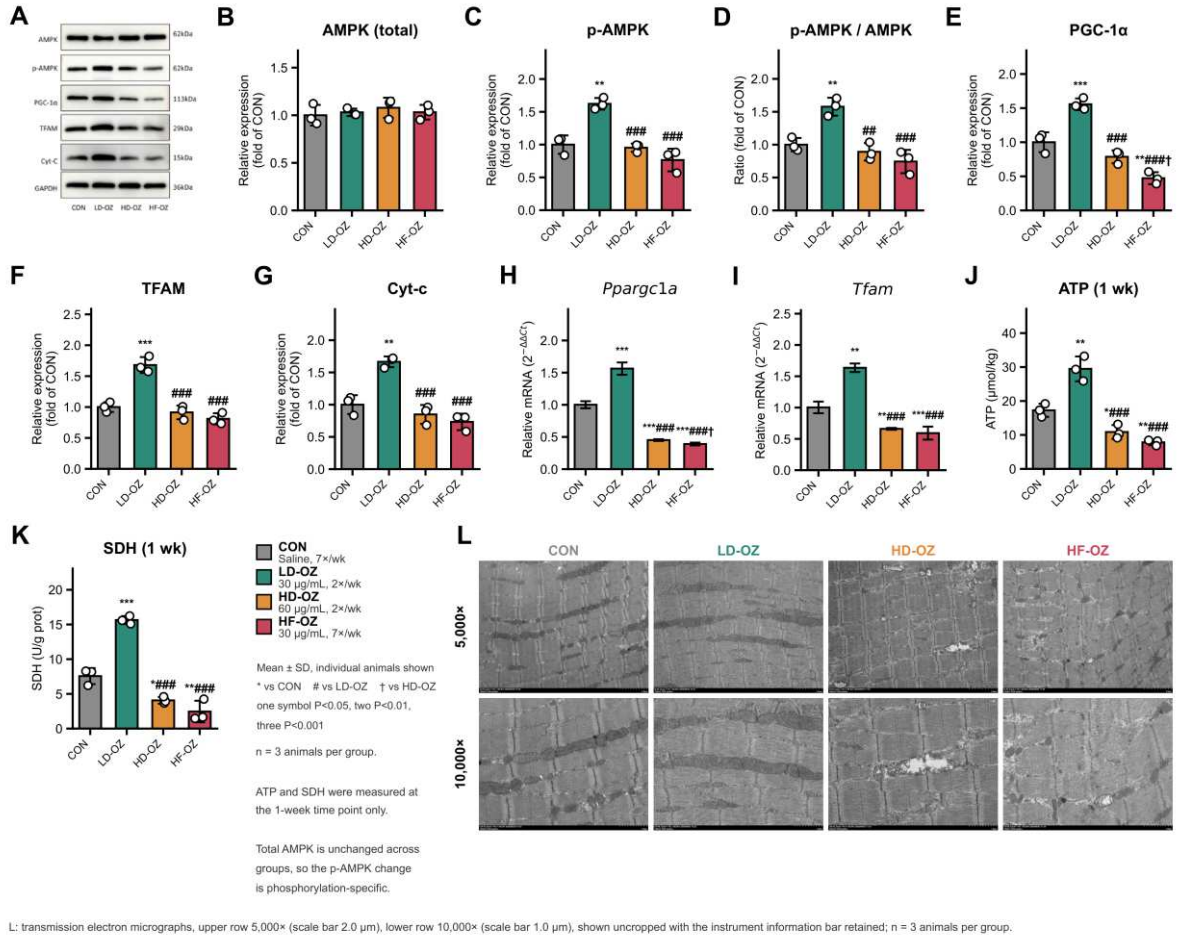
Low exposure was associated with a mitochondrial adaptation-related profile

LD-OZ was associated with coordinated changes in mitochondrial-related endpoints. p-AMPK increased without a corresponding change in total AMPK, and the p-AMPK/total AMPK ratio remained elevated. PGC-1α, TFAM, and cytochrome c increased at the protein level, while Ppargc1a and Tfam transcripts showed a concordant pattern. At week 1, ATP was 71% higher and succinate dehydrogenase activity was 107% higher than in CON. Electron microscopy showed relatively regular myofibrillar alignment and closely apposed mitochondria in LD-OZ(Fig. 3).

Atrogin-1 protein and Fbxo32 transcript were lower in LD-OZ, whereas MuRF1 and total ubiquitinated protein were not significantly changed. Together, these findings describe a mitochondrial adaptation-

associated profile accompanied by a selective reduction in one atrophy-related marker. They do not establish the full causal sequence of mitochondrial biogenesis.

Insert Fig. 3 here



L: transmission electron micrographs, upper row 5,000× (scale bar 2.0 μm), lower row 10,000× (scale bar 1.0 μm), shown uncropped with the instrument information bar retained; n = 3 animals per group.

Figure 3. Mitochondrial-related endpoints. (A) Representative immunoblots. (B) Total AMPK. (C) p-AMPK. (D) p-AMPK/total AMPK. (E) PGC-1α. (F) TFAM. (G) Cytochrome c. (H, I) Ppargc1a and Tfam transcripts. (J, K) ATP and succinate dehydrogenase activity at week 1. (L) Representative transmission electron micrographs at 5000× and 10,000×. n = 3 animals per group for molecular and biochemical assays and electron microscopy.

Higher exposure was associated with oxidative changes and altered glutathione-related measures

The higher-exposure groups showed a redox profile distinct from LD-OZ. Muscle 8-OHdG and MDA were elevated in HD-OZ and HF-OZ, with group differences evident early and no significant group-by-time interaction. T-GSH declined across the sampling period, and GSSG was also lower in the higher-exposure groups(Fig. 4). Serum CK and LDH increased over time and reached their highest values in HF-OZ at week 7, whereas LD-OZ remained closer to control values.

These measures showed different temporal patterns: oxidative modification, glutathione-related measures, and serum enzyme leakage did not change identically. Because recovery kinetics between

injections were not measured directly, the findings support an exposure-associated redox burden but do not establish why the changes persisted or progressed.

Insert Fig. 4 here

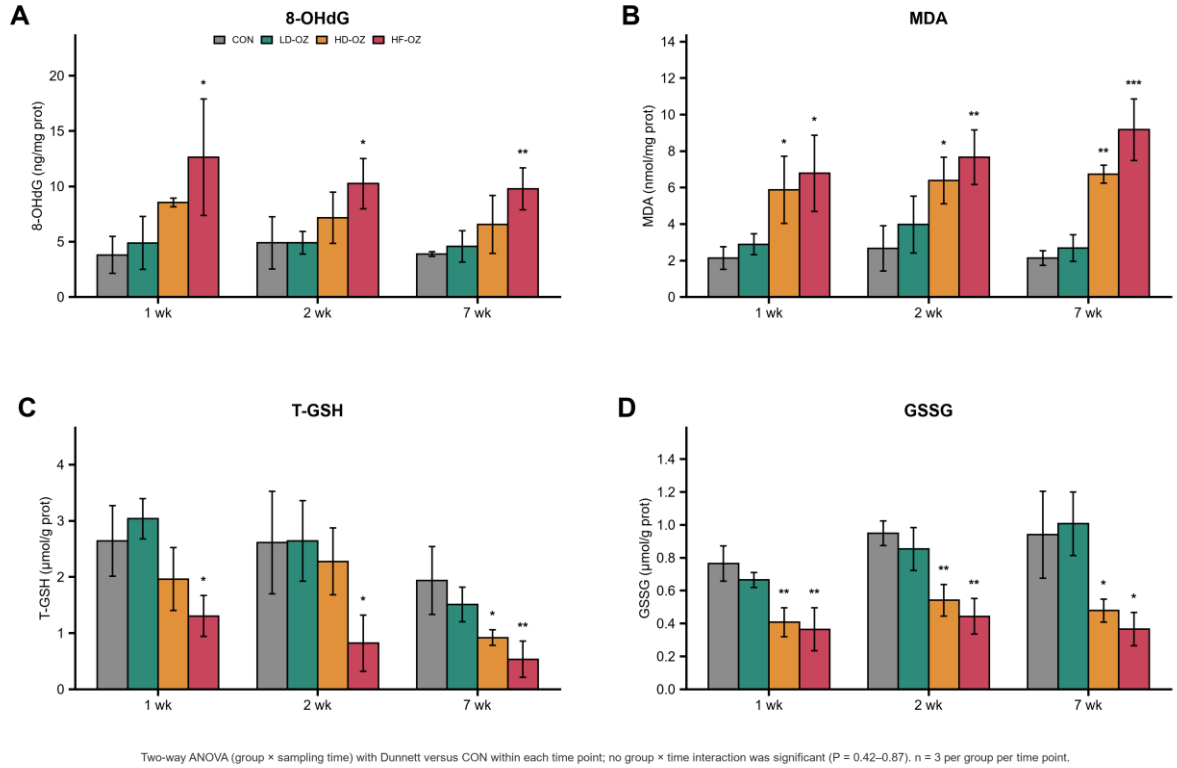


Figure 4. Oxidative-stress and antioxidant-reserve markers at weeks 1, 2, and 7. (A) 8-OHdG. (B) MDA. (C) T-GSH. (D) GSSG. Data are mean ± SD; n = 3 per group per time point. Two-way ANOVA was followed by within-time-point comparisons against CON.

Higher exposure was accompanied by NLRP3–GSDMD-associated inflammatory changes

Compared with CON, HD-OZ and HF-OZ showed higher abundance of NLRP3, ASC, pro-caspase-1, cleaved caspase-1, GSDMD-N, and cleaved IL-1β. Muscle IL-1β and TNF-α also showed strong group effects. GSDMD-N-positive area increased most clearly in HF-OZ, and TUNEL-positive nuclei were markedly more frequent in HD-OZ and HF-OZ. LD-OZ did not show a comparable increase across the inflammasome-related protein panel(Fig. 5).

The combined changes in inflammasome-related proteins, GSDMD-N, and inflammatory cytokines are consistent with an NLRP3–GSDMD-associated pyroptosis-related response. Because the study did not include pathway inhibition, genetic manipulation, or cell-type-specific localization, these results are pathway-associated evidence rather than proof that NLRP3–GSDMD signalling caused the observed fibre atrophy.

Insert Fig. 5 here

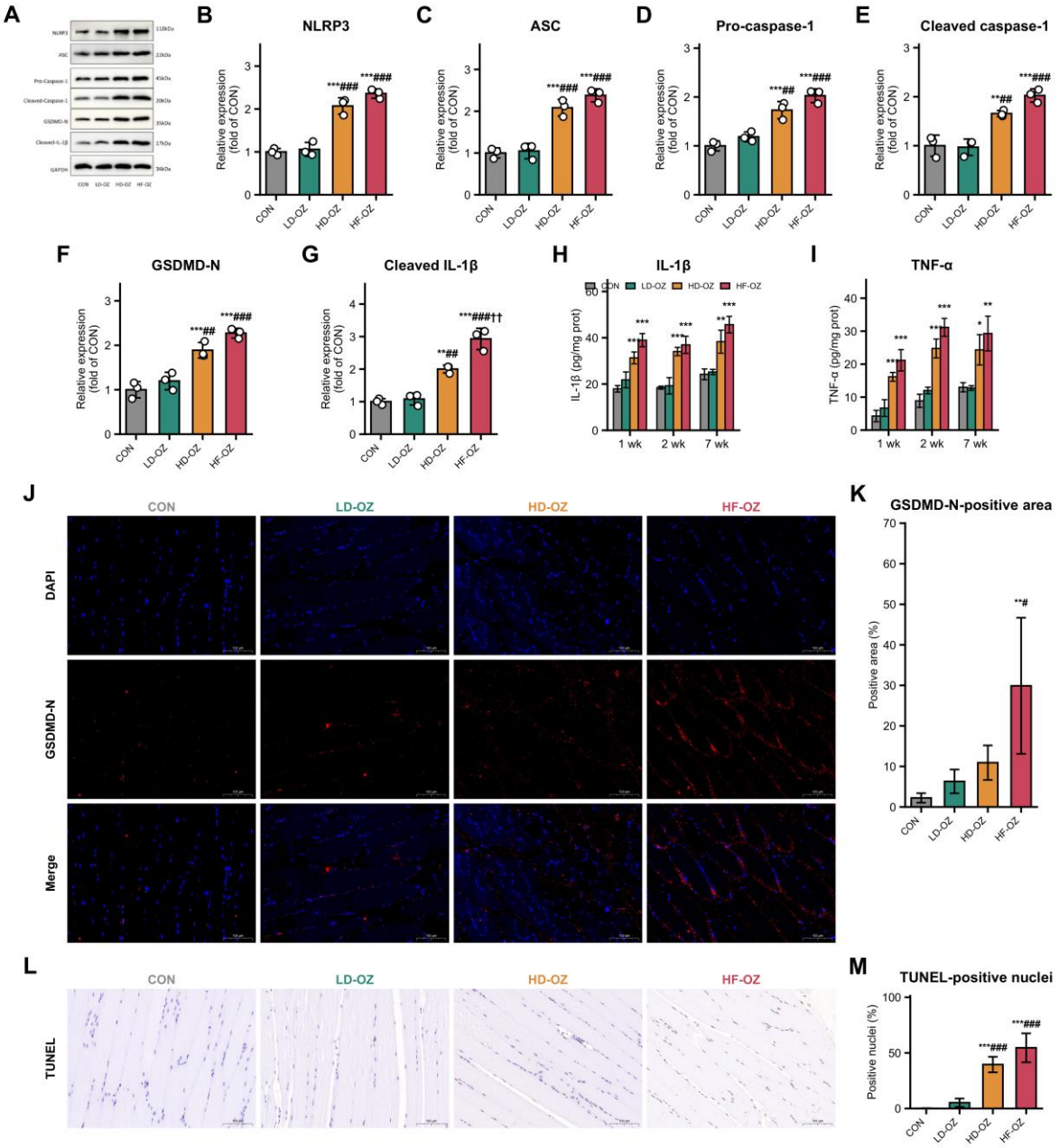


Figure 5. NLRP3–GSDMD-associated inflammatory and pyroptosis-related markers. (A) Representative immunoblots. (B–G) Densitometry of NLRP3, ASC, pro-caspase-1, cleaved caspase-1, GSDMD-N, and cleaved IL-1β. (H, I) Muscle IL-1β and TNF-α. (J, K) GSDMD-N immunofluorescence and positive-area quantification. (L, M) TUNEL staining and positive-nuclei quantification. Scale bars, 100 μm.

Higher exposure was accompanied by proteolysis-related and muscle-injury-associated changes

The injury-associated groups also showed changes in muscle protein-turnover markers. MuRF1, atrogin-1, total ubiquitinated protein, Trim63, and Fbxo32 were higher in HD-OZ and HF-OZ than in CON. In contrast, atrogin-1 was lower in LD-OZ. MuRF1-positive area increased across the regimens. Serum CK and LDH showed time-dependent increases, particularly in HF-OZ(Fig. 6).

Electron microscopy in HD-OZ and HF-OZ showed sarcomeric disorganization, widened Z-line spacing, swollen mitochondria, and disrupted cristae. PGC-1α was lower in the higher-exposure groups, whereas not all other mitochondrial markers differed significantly from CON. Together, the findings support a higher-exposure phenotype characterized by structural injury and proteolysis-related molecular changes.

Insert Fig. 6 here

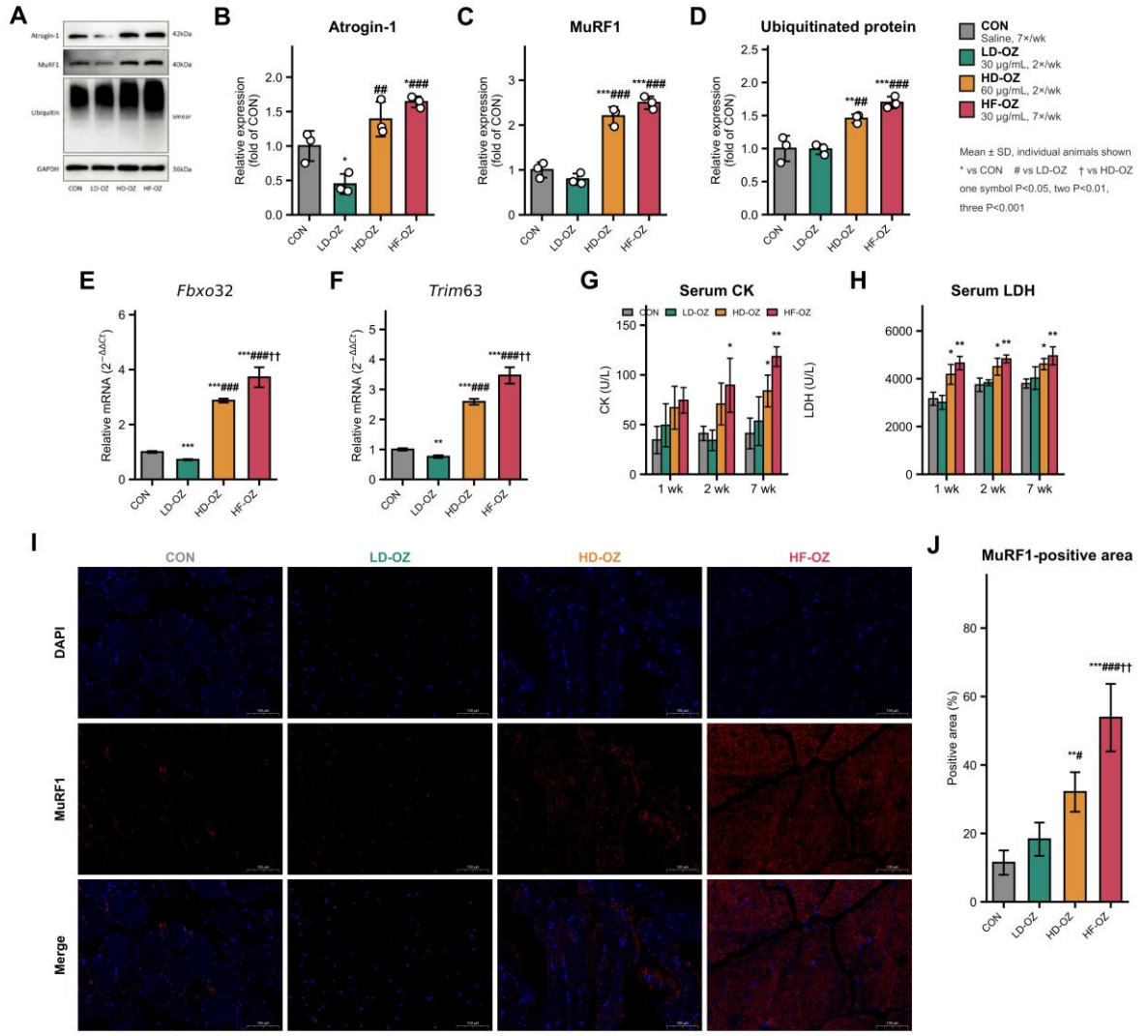


Figure 6. Proteolysis-related and muscle-injury-associated endpoints. (A) Representative immunoblots. (B–D) Atrogin-1, MuRF1, and ubiquitinated protein. (E, F) Fbxo32 and Trim63 transcripts. (G, H) Serum CK and LDH at weeks 1, 2, and 7. (I, J) MuRF1 immunofluorescence and positive-area quantification. Scale bars, 100 μm.

Response patterns differed by endpoint and over time

Across endpoints, ATP, succinate dehydrogenase activity, PGC-1α, grip strength, and atrogin-1 showed opposing patterns between LD-OZ and the higher-exposure groups. p-AMPK, TFAM, and cytochrome c showed an ascending low-exposure pattern without a statistically significant reduction below CON in HF-OZ. Inflammasome-related markers, MuRF1, ubiquitinated protein, fibre area, collagen area, and rotarod latency were predominantly altered in the higher-exposure groups.

The response classes summarized in Figure 7 describe the patterns observed among the tested regimens; they do not establish a common quantitative threshold or imply that HD-OZ and HF-OZ are biologically equivalent. The time courses also differed among endpoints: inflammatory and redox markers did not follow identical trajectories, while glutathione-related measures and enzyme leakage showed progressive changes during treatment.

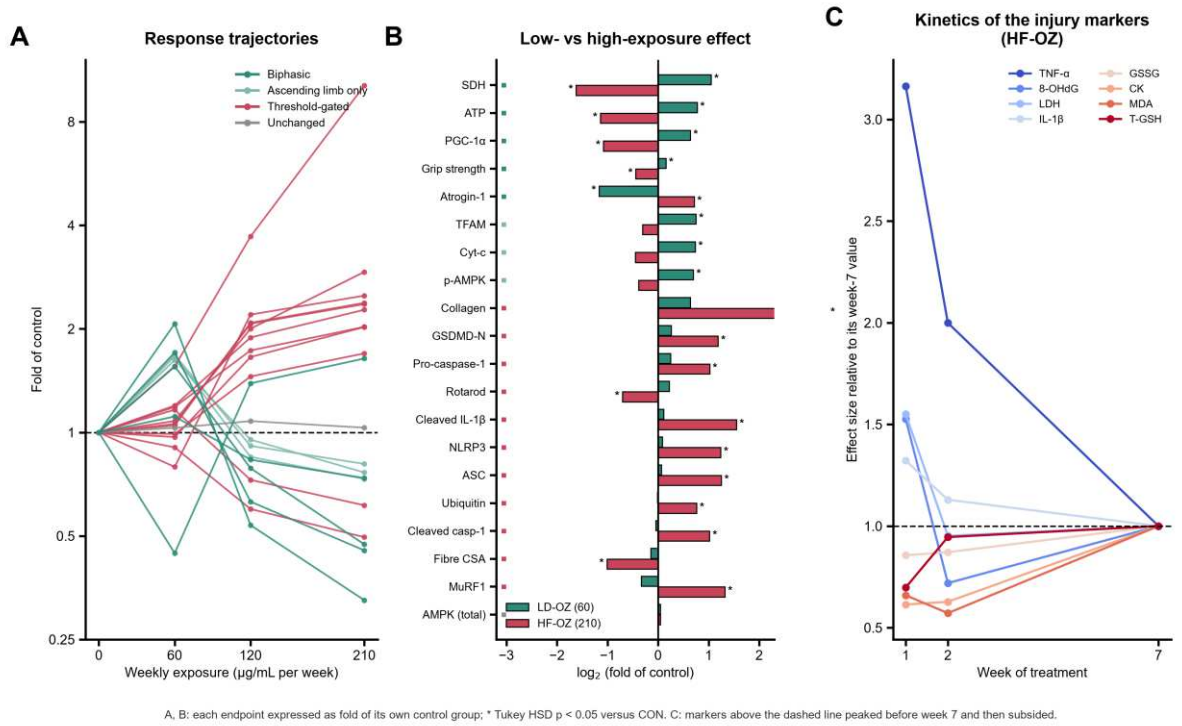


Figure 7. Integrated response patterns and temporal relationships. (A) Response trajectories across the tested weekly exposures. (B) Low- versus high-exposure effects on a $\log_2$ scale. (C) Time courses of selected injury-associated markers in HF-OZ. Classifications summarize observed endpoint patterns and do not establish a universal quantitative threshold.

Discussion

Across the regimens tested, intramuscular ozone was associated with concentration-, frequency-, and endpoint-dependent responses in rat skeletal muscle. The 30 μg/mL twice-weekly regimen (LD-OZ) showed a comparatively favourable profile, including higher grip strength, ATP, and succinate dehydrogenase activity, lower atrogin-1, and relatively preserved muscle architecture. In contrast, doubling the concentration or increasing administration frequency was associated with functional impairment, oxidative changes, inflammatory and proteolysis-related markers, and structural abnormalities. This pattern is compatible with a hormesis-like response over the tested range, but it does not establish a biphasic curve or a defined therapeutic window. Lower concentrations and less frequent schedules were not tested, so the lower boundary of any adaptive range remains unknown [14,22].

Exposure parameters were not equally associated with every endpoint. In the two-week screen, the quadriceps-to-body-weight ratio tracked injection frequency more clearly than ozone concentration, and a simple product of concentration and frequency did not improve model fit over frequency-based descriptions. The absence of a detectable concentration effect on gross muscle mass should not be interpreted as evidence that concentration is biologically irrelevant. In the main experiment, gross muscle mass did not clearly identify the HD-OZ phenotype, whereas grip strength, fibre cross-sectional area, and inflammasome- and proteolysis-related markers indicated injury-associated changes. Thus, gross muscle mass alone may be less sensitive than functional, structural, and molecular measures for detecting local muscle changes [23–26].

The difference between gross muscle mass and the other endpoints may reflect the biological components captured by each measure. Wet weight aggregates contractile tissue, connective tissue, extracellular matrix, and water content, while extracellular-matrix organization also contributes to tissue mechanics and force transmission [27,30]. Early or moderate myofibre injury may therefore affect force production, energy metabolism, or fibre morphology before total muscle weight changes detectably. The relationships between mitochondrial dysfunction, muscle quality, and injury support evaluating muscle function and structure alongside gross mass [28–29]. In this study, the combined functional, histological, biochemical, and molecular endpoints provided a broader description of regimen-associated responses than muscle mass alone.

Several injury-associated outcomes appeared nonlinear across the tested regimens. HD-OZ and HF-OZ showed broadly similar reductions in grip strength, rotarod latency, and fibre cross-sectional area, and similar changes in several inflammasome-related proteins, despite different nominal weekly exposures. Cleaved IL-1β was an exception, continuing to increase in HF-OZ. This pattern could reflect endpoint-specific plateau-like responses, but it does not establish saturation or a switch-like threshold. Redox responses may be nonlinear and context dependent [14,22,31–32], while inflammasome assembly and IL-1β maturation involve multiple regulatory steps [34]. The limited number of concentration–frequency combinations and small endpoint-specific samples preclude a definitive exposure–response model; additional intermediate regimens and prespecified nonlinear analyses would be required [33].

Atrogin-1 and MuRF1 did not respond identically. Atrogin-1 was lower in LD-OZ, while MuRF1 did not show a comparable reduction; both markers increased under higher exposure, particularly at the transcript level. Differential regulation through mTOR/S6K1-, FoxO-, and inflammation-associated pathways is biologically plausible [35–36], and inflammatory signalling can interact with muscle atrophy pathways [37,39]. However, the upstream activities of NF-κB, FoxO, and other regulators were not directly measured. Atrogin-1 and MuRF1 should therefore be interpreted as markers associated with protein-turnover regulation, not as direct measurements of overall proteolytic flux [38,40].

The differences between transcript and protein responses also warrant restraint. MuRF1 and atrogin-1 transcripts increased more consistently than their protein abundance at higher exposure. Possible explanations include post-transcriptional regulation, altered translation, protein stability, turnover, or a ceiling effect, but the present data cannot distinguish among them [41,44–45]. E3 ligase abundance should not be equated with bulk proteasome activity or total protein degradation: ubiquitination can have proteolytic and non-proteolytic functions and is regulated by deubiquitinases [42–43,46]. Measurements of protein turnover, proteasome activity, translation, and ubiquitination status would be needed to resolve this discordance and strengthen mechanistic interpretation [41–46].

Inflammatory and redox endpoints showed different temporal profiles. Several inflammatory markers, especially TNF-α, were most prominent at week 1 and declined thereafter, whereas lipid peroxidation, glutathione-related changes, and serum enzyme leakage were more pronounced by week 7. Distinct time courses have been reported in other muscle-stress and injury settings [47–48,51]. A decline in inflammatory markers does not necessarily indicate complete tissue recovery, because inflammatory resolution can coexist with ongoing remodelling or injury [48]. The present time-course data show temporal association, not that early inflammation caused later redox or structural changes. Intervention studies targeting inflammatory and redox pathways would be needed to test causal relationships; protective effects reported in other muscle-injury models do not demonstrate the same mechanism in this ozone model [49–50,52].

The LD-OZ group showed the most consistent mitochondrial adaptation-related pattern. Increases in p-AMPK, PGC-1α, TFAM, cytochrome c, Ppargc1a, Tfam, ATP, and succinate dehydrogenase activity were compatible with an AMPK–PGC-1α–TFAM-associated response [16,53–54]. Higher p-AMPK without a change in total AMPK is consistent with increased phosphorylation, but does not by itself establish complete downstream pathway activation [16,55]. The concordant changes in proteins, transcripts, ATP, and enzyme activity suggest that the pattern extended beyond a single marker. Nevertheless, pathway inhibition, genetic manipulation, and direct mitochondrial-respiration measurements were not performed; the data therefore support mechanistic associations rather than demonstrating that this signalling axis mediated the response [16,53,56].

The translational implication is not a clinical dose recommendation. Rather, the results suggest that ozone concentration and administration frequency should be evaluated as distinct regimen parameters when studying local muscle safety [1,57]. Direct extrapolation to human intramuscular or paravertebral procedures is not justified because species anatomy, tissue geometry, injection volume, local distribution, and exposure kinetics may differ substantially [59]. Clinical evidence and treatment schedules remain heterogeneous, and the current rat findings should be treated as hypothesis-generating rather than prescriptive [1,5,57–58]. The findings also support using functional, histological, biochemical, and

molecular outcomes alongside gross muscle mass. Responses following systemic ozone administration or other delivery routes should not be assumed to be interchangeable with local intramuscular exposure [1,57,59].

Several limitations affect interpretation. First, the lower boundary of a possible adaptive range cannot be defined because lower concentrations and less frequent schedules were not tested. Second, the limited set of concentration–frequency combinations and small endpoint-specific sample sizes prevent robust characterization of the response surface or confirmation of a biphasic hormetic curve [32]. Third, causal involvement of the AMPK–PGC-1α–TFAM axis, inflammasome signalling, and proteolytic pathways was not tested directly. Fourth, only healthy male rats were studied, limiting generalization to females, aged animals, diseased muscle, or human patients with chronic musculoskeletal disorders [60–61]. Fifth, endpoint-specific sampling schedules limit direct temporal alignment across molecular, functional, and histological measures. Finally, nominal ozone concentration does not define the tissue exposure achieved after injection; local distribution, retention, and post-injection reactions remain uncharacterized [62].

A further limitation is the absence of frequency-matched procedural controls for all ozone regimens. In the main experiment, saline controls received seven intramuscular injections per week, matching HF-OZ but not the twice-weekly LD-OZ and HD-OZ regimens. Comparisons of the twice-weekly ozone groups with CON may therefore reflect differences in needle insertion, handling, or anaesthesia as well as differences in the injected preparation. The LD-OZ versus HD-OZ comparison matched injection frequency and is consequently more informative about concentration-associated differences within the tested design. HF-OZ and CON were frequency-matched, but saline was not a gas-matched oxygen–ozone control. Comparisons between LD-OZ and HF-OZ cannot isolate ozone frequency from repeated procedural exposure. These design constraints also temper interpretation of frequency-associated findings in the screening stage. Future studies should include frequency-matched saline groups, oxygen-only controls, and appropriate sham procedures. Accordingly, the present findings are best described as regimen-associated responses, not definitive independent causal effects of ozone concentration or administration frequency.A proposed working model integrating these regimen-associated responses is presented in Fig. 8.

Insert Fig. 8 here

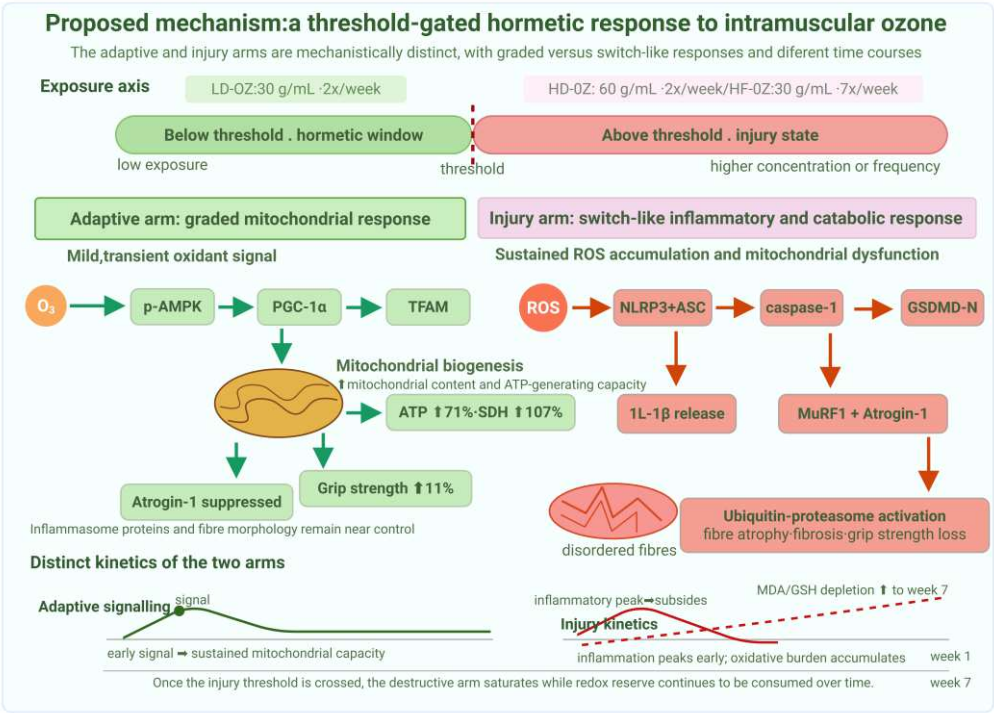


Figure 8. Proposed working model. The diagram summarizes the association of the LD-OZ regimen with mitochondrial adaptation-related endpoints and of higher-exposure regimens with oxidative, inflammatory, proteolysis-related, and structural injury markers. Arrows represent a working hypothesis and do not establish causal direction.

Conclusions

In this rat model, intramuscular ozone regimens were associated with concentration-, frequency-, and endpoint-dependent skeletal-muscle responses. The 30 μg/mL twice-weekly regimen was associated with a comparatively favourable profile, including improved grip strength, higher ATP and succinate dehydrogenase activity, changes in mitochondrial adaptation-related markers, and lower atrogin-1. Higher concentration or more frequent administration was associated with oxidative, inflammatory, proteolysis-related, structural, and functional injury-associated changes. Gross muscle mass was less sensitive than functional, histological, biochemical, and molecular endpoints for identifying the HD-OZ phenotype. The findings are compatible with a hormesis-like exposure–response pattern within the tested regimens, but do not establish a defined threshold, causal pathway, or clinical dosing recommendation.

Declarations

Ethics approval and consent to participate: The animal study protocol was approved by the Ethics Committee of the Animal Experimental Center of Henan University of Chinese Medicine (approval no. IACUC-202603021). The study was reported in accordance with ARRIVE 2.0.

Consent for publication: Not applicable.

Availability of data and materials: The data supporting the findings are presented in the article and its figures. The underlying data are held by the first author and may be requested from the corresponding author.

Competing interests: The authors declare that they have no competing interests.

Funding: This research was supported by the Traditional Chinese Medicine Discipline Construction Project of the Characteristic Backbone Disciplines of Henan Province, China (Grant No. STG-ZYX02-202115).

Authors' contributions: Conceptualization: M.L. and Y.Z.; methodology: M.L. and Y.Z.; formal analysis: Y.F. and T.Z.; data curation: Y.F. and T.Z.; visualization: W.L., J.S., and M.L.; writing—original draft: M.L.; writing—review and editing: M.L., J.S., and Y.F.; supervision: Y.Z.; project administration: Y.Z.; funding acquisition: Y.Z. All authors read and approved the final manuscript.

Acknowledgements: ChatGPT (OpenAI) was used to assist with language editing and manuscript restructuring. It was not used to generate experimental data or modify the reported results. The authors are responsible for checking the accuracy and integrity of the final manuscript.

Abbreviations

ALT, alanine aminotransferase; AMPK, AMP-activated protein kinase; ATP, adenosine triphosphate; AST, aspartate aminotransferase; BUN, blood urea nitrogen; CK, creatine kinase; CON, saline control; Cr, creatinine; GSDMD, gasdermin D; HF-OZ, high-frequency ozone; HD-OZ, high-dose ozone; LDH, lactate dehydrogenase; LD-OZ, low-dose ozone; MDA, malondialdehyde; NLRP3, NOD-, LRR- and pyrin domain-containing protein 3; PGC-1α, peroxisome proliferator-activated receptor gamma coactivator 1-alpha; SDH, succinate dehydrogenase; T-GSH, total glutathione; TFAM, mitochondrial transcription factor A.

References

1. Jeyaraman, M., Jeyaraman, N., Ramasubramanian, S., Balaji, S., Nallakumarasamy, A., Patro, B.P., Migliorini, F. Ozone Therapy in Musculoskeletal Medicine: A Comprehensive Review. Eur. J. Med. Res. 2024;29:398. https://doi.org/10.1186/s40001-024-01976-4.

2. Kelekis, A., Bonaldi, G., Cianfoni, A., Filippiadis, D., Scarone, P., Bernucci, C., Hooper, D.M., Benhabib, H., Murphy, K., Buric, J. Intradiscal Oxygen–Ozone Chemonucleolysis versus Microdiscectomy for Lumbar Disc Herniation Radiculopathy: A Non-Inferiority Randomized Control Trial. Spine J. 2022;22:895–909. https://doi.org/10.1016/j.spinee.2021.11.017.

3. Sconza, C., Di Matteo, B., Queirazza, P., Dina, A., Amenta, R., Respizzi, S., Massazza, G., Ammendolia, A., Kon, E., de Sire, A. Ozone Therapy versus Hyaluronic Acid Injections for Pain Relief in Patients with Knee Osteoarthritis: Preliminary Findings on Molecular and Clinical Outcomes from a Randomized Controlled Trial. Int. J. Mol. Sci. 2023;24:8788. https://doi.org/10.3390/ijms24108788.

4. Korkmaz, N., Örücü Atar, M., Uyar Köylü, S., Gümrük Aslan, S., Tezen, Ö., Kesikburun, S. Comparison of the Efficacy of Oxygen–Ozone and Lidocaine Injections in the Treatment of Myofascial Pain Syndrome: A Randomized Clinical Trial. Turk. J. Phys. Med. Rehabil. 2023;69:294–302. https://doi.org/10.5606/tftrd.2023.11516.

5. Lino, V.T.S., Marinho, D.S., Rodrigues, N.C.P., Andrade, C.A.F. Efficacy and Safety of Ozone Therapy for Knee Osteoarthritis: An Umbrella Review of Systematic Reviews. Front. Physiol. 2024;15:1348028. https://doi.org/10.3389/fphys.2024.1348028

6. Lietz-Kijak, D., Skibicka, K., Skomro, P., Brodkiewicz, A., Budkowska, M., Kijak, K., Gronwald, H., Kijak, K., Szczegielniak, J., Bogacz, K., Bitenc-Jasiejko, A., Szczucka, L., Garstka, A.A., Wójcik, M. Medical Ozone: Mechanisms, Biological Effects and Clinical Evidence-A Narrative Review. Front. Med. 2026;13:1859221. https://doi.org/10.3389/fmed.2026.1859221

7. Guo, H.-Z., Yu, S.-L., Chen, H.-W. Major Ozonated Autoheamotherapy Alleviates Skeletal Muscle Ischemia/Reperfusion Injury by Regulating Nrf2/HO-1 Pathway. Kaohsiung J. Med. Sci. 2025;41:e70039. https://doi.org/10.1002/kjm2.70039

8. de Souza, K.B.R., Guerra, L.R.A., Guerreiro, M.L.S., Casais-e-Silva, L.L., Aguiar, M.C. Nociceptive and Histomorphometric Evaluation of the Effects of Ozone Therapy on the Rat Masseter Muscle in a Carrageenan Model of Myofascial Pain. Arch. Oral Biol. 2024;160:105893. https://doi.org/10.1016/j.archoralbio.2024.105893

9. Rania, V., Marcianò, G., Casarella, A., Vocca, C., Palleria, C., Calabria, E., Spaziano, G., Citraro, R., De Sarro, G., Monea, F., Gallelli, L. Oxygen–Ozone Therapy in Cervicobrachial Pain: A Real-Life Experience. J. Clin. Med. 2023;12:248. https://doi.org/10.3390/jcm12010248

10. Latini, E., Nusca, S.M., Curci, E.R., Boaretto, D., Santoboni, F., Trischitta, D., Vetrano, M., Vulpiani, M.C. Intramuscular Paravertebral Oxygen–Ozone Therapy for Chronic Neck Pain and Low Back Pain: Evaluation of 6-Month Clinical Outcomes. Med. Gas Res. 2024;14:6-11. https://doi.org/10.4103/2045-9912.374388

11. Aragon, A.A., Tipton, K.D., Schoenfeld, B.J. Age-Related Muscle Anabolic Resistance: Inevitable or Preventable? Nutr. Rev. 2023;81:441-454. https://doi.org/10.1093/nutrit/nuac062

12. Smith, C., Woessner, M.N., Sim, M., Levinger, I. Sarcopenia Definition: Does It Really Matter? Implications for Resistance Training. Ageing Res. Rev. 2022;78:101617. https://doi.org/10.1016/j.arr.2022.101617

13. Cenci, A., Macchia, I., La Sorsa, V., Sbarigia, C., Di Donna, V., Pietraforte, D. Mechanisms of Action of Ozone Therapy in Emerging Viral Diseases: Immunomodulatory Effects and Therapeutic Advantages with Reference to SARS-CoV-2. Front. Microbiol. 2022;13:871645. https://doi.org/10.3389/fmicb.2022.871645

14. Chirumbolo, S., Tirelli, U., Franzini, M., Pandolfi, S., Ricevuti, G., Vaiano, F., Valdenassi, L. Ozone in the Adjunct Medical Treatment: The Round Personality of a Molecule with Hormetic Properties. Hum. Exp. Toxicol. 2023;42:9603271231218926. https://doi.org/10.1177/09603271231218926

15. Borrelli, E. Ozone Therapy as a Redox-Modulating Strategy in Degenerative Musculoskeletal Diseases: A Clinical–Mechanistic Review. J. Clin. Med. 2026;15:6065. https://doi.org/10.3390/jcm15156065

16. Reisman, E.G., Hawley, J.A., Hoffman, N.J. Exercise-Regulated Mitochondrial and Nuclear Signalling Networks in Skeletal Muscle. Sports Med. 2024;54:1097–1119. https://doi.org/10.1007/s40279-024-02007-2

17. Slavin, M.B., Khemraj, P., Hood, D.A. Exercise, Mitochondrial Dysfunction and Inflammasomes in Skeletal Muscle. Biomed. J. 2024;47:100636. https://doi.org/10.1016/j.bj.2023.100636

18. Pelinsari, S.M., Sarandy, M.M., Vilela, E.F., Novaes, R.D., Schlamb, J., Gonçalves, R.V. Ozone Exposure Controls Oxidative Stress and the Inflammatory Process of Hepatocytes in Murine Models. Antioxidants 2024;13:212. https://doi.org/10.3390/antiox13020212

19. Wu, J., Ding, P., Wu, H., Yang, P., Guo, H., Tian, Y., Meng, L., Zhao, Q. Sarcopenia: Molecular Regulatory Network for Loss of Muscle Mass and Function. Front. Nutr. 2023;10:1037200. https://doi.org/10.3389/fnut.2023.1037200

20. Yang, H., Xiao, X., Chen, G., Chen, X., Gao, T., Xu, L. Preliminary Study on the Effect of Ozone Exposure on Blood Glucose Level in Rats. Technol. Health Care 2023, 31 (Suppl. 1), 303–311. https://doi.org/10.3233/THC-236026

21. Zhao, J., Yang, Q., Liu, Z., Xu, P., Tian, L., Yan, J., Li, K., Lin, B., Bian, L., Xi, Z., Liu, X. The Impact of Subchronic Ozone Exposure on Serum Metabolome and the Mechanisms of Abnormal Bile Acid and Arachidonic Acid Metabolisms in the Liver. Ecotoxicol. Environ. Saf. 2023;252:114573. https://doi.org/10.1016/j.ecoenv.2023.114573

22. Inguscio, C.R., Dalla Pozza, E., Dando, I., Boschi, F., Tabaracci, G., Angelini, O., Picotti, P.M., Malatesta, M., Cisterna, B. Mitochondrial Features of Mouse Myoblasts Are Finely Tuned by Low Doses of Ozone: The Evidence In Vitro. Int. J. Mol. Sci. 2023;24:8900. https://doi.org/10.3390/ijms24108900.

23. Naimo, M.A., Varanoske, A.N., Hughes, J.M., Pasiakos, S.M. Skeletal Muscle Quality: A Biomarker for Assessing Physical Performance Capabilities in Young Populations. Front. Physiol. 2021;12:706699. https://doi.org/10.3389/fphys.2021.706699.

24. Rostron, Z.P., Green, R.A., Kingsley, M., Zacharias, A. Associations between Measures of Physical Activity and Muscle Size and Strength: A Systematic Review. Arch. Rehabil. Res. Clin. Transl. 2021;3:100124. https://doi.org/10.1016/j.arrct.2021.100124.

25. Dent, E., Woo, J., Scott, D., Hoogendijk, E.O. Sarcopenia Measurement in Research and Clinical Practice. Eur. J. Intern. Med. 2021;90:1–9. https://doi.org/10.1016/j.ejim.2021.06.003.

26. Yin, L., Li, N., Jia, W., Wang, N., Liang, M., Yang, X., Du, G. Skeletal Muscle Atrophy: From Mechanisms to Treatments. Pharmacol. Res. 2021;172:105807. https://doi.org/10.1016/j.phrs.2021.105807.

27. Wohlgemuth, R.P., Brashear, S.E., Smith, L.R. Alignment, Cross Linking, and Beyond: A Collagen Architect's Guide to the Skeletal Muscle Extracellular Matrix. Am. J. Physiol. Cell Physiol. 2023;325:C1017–C1030. https://doi.org/10.1152/ajpcell.00287.2023.

28. Chen, X., Ji, Y., Liu, R., Zhu, X., Wang, K., Yang, X., Liu, B., Gao, Z., Huang, Y., Shen, Y., Liu, H., Sun, H. Mitochondrial Dysfunction: Roles in Skeletal Muscle Atrophy. J. Transl. Med. 2023;21:503. https://doi.org/10.1186/s12967-023-04369-z.

29. Edouard, P., Reurink, G., Mackey, A.L., Lieber, R.L., Pizzari, T., Järvinen, T.A.H., Gronwald, T., Hollander, K. Traumatic Muscle Injury. Nat. Rev. Dis. Primers 2023;9:56. https://doi.org/10.1038/s41572-023-00469-8.

30. Mavropalias, G., Boppart, M., Usher, K.M., Grounds, M.D., Nosaka, K., Blazevich, A.J. Exercise Builds the Scaffold of Life: Muscle Extracellular Matrix Biomarker Responses to Physical Activity, Inactivity, and Aging. Biol. Rev. Camb. Philos. Soc. 2023;98:481–519. https://doi.org/10.1111/brv.12916.

31. Skaperda, Z., Tekos, F., Vardakas, P., Nepka, C., Kouretas, D. Reconceptualization of Hormetic Responses in the Frame of Redox Toxicology. Int. J. Mol. Sci. 2022;23(1):49. https://doi.org/10.3390/ijms23010049.

32. Bondy, S.C. The Hormesis Concept: Strengths and Shortcomings. Biomolecules 2023;13(10):1512. https://doi.org/10.3390/biom13101512.

33. Kappenberg, F., Duda, J.C., Schürmeyer, L., Gül, O., Brecklinghaus, T., Hengstler, J.G., Schorning, K., Rahnenführer, J. Guidance for Statistical Design and Analysis of Toxicological Dose–Response Experiments, Based on a Comprehensive Literature Review. Arch. Toxicol. 2023;97(10):2741–2761. https://doi.org/10.1007/s00204-023-03561-w.

34. Xu, J., Núñez, G. The NLRP3 Inflammasome: Activation and Regulation. Trends Biochem. Sci. 2023;48(4):331–344. https://doi.org/10.1016/j.tibs.2022.10.002.

35. Nishimura, Y., Chunthorng-Orn, J., Lord, S., Musa, I., Dawson, P., Holm, L., Lai, Y.-C. Ubiquitin E3 Ligase Atrogin-1 Protein Is Regulated via the Rapamycin-Sensitive mTOR-S6K1 Signaling Pathway in C2C12 Muscle Cells. Am. J. Physiol. Cell Physiol. 2022;323(1):C215–C225. https://doi.org/10.1152/ajpcell.00384.2021.

36. Vilchinskaya, N., Altaeva, E., Lomonosova, Y. Gaining Insight into the Role of FoxO1 in the Progression of Disuse-Induced Skeletal Muscle Atrophy. Adv. Biol. Regul. 2022;85:100903. https://doi.org/10.1016/j.jbior.2022.100903.

37. Ji, Y., Li, M., Chang, M., Liu, R., Qiu, J., Wang, K., Deng, C., Shen, Y., Zhu, J., Wang, W., et al. Inflammation: Roles in Skeletal Muscle Atrophy. Antioxidants 2022;11:1686. https://doi.org/10.3390/antiox11091686.

38. Gellhaus, B., Böker, K.O., Schilling, A.F., Saul, D. Therapeutic Consequences of Targeting the IGF-1/PI3K/AKT/FOXO3 Axis in Sarcopenia: A Narrative Review. Cells 2023;12:2787. https://doi.org/10.3390/cells12242787.

39. Wilburn, D., Ismaeel, A., Machek, S., Fletcher, E., Koutakis, P. Shared and Distinct Mechanisms of Skeletal Muscle Atrophy: A Narrative Review. Ageing Res. Rev. 2021;71:101463. https://doi.org/10.1016/j.arr.2021.101463.

40. Gouvêa de Souza, A.L., Rosa Alves, A.L., Guerra Martinez, C., Costa de Sousa, J., Kurtenbach, E. Biomarkers of Skeletal Muscle Atrophy Based on Atrogenes Evaluation: A Systematic Review and Meta-Analysis Study. Int. J. Mol. Sci. 2025;26:3516. https://doi.org/10.3390/ijms26083516.

41. Mei, H., Boom, J., El Abdellaoui, S., Abdelmohsen, K., Munk, R., Martindale, J.L., Kloet, S., Kielbasa, S.M., Sharp, T.H., Gorospe, M., Raz, V. Alternative Polyadenylation Utilization Results in Ribosome Assembly and mRNA Translation Deficiencies in a Model for Muscle Aging. J. Gerontol. A Biol. Sci. Med. Sci. 2022;77(6):1130–1140. https://doi.org/10.1093/gerona/glac058.

42. Hughes, D.C., Goodman, C.A., Baehr, L.M., Gregorevic, P., Bodine, S.C. A Critical Discussion on the Relationship between E3 Ubiquitin Ligases, Protein Degradation, and Skeletal Muscle Wasting: It's Not That Simple. Am. J. Physiol. Cell Physiol. 2023;325(6):C1567–C1582. https://doi.org/10.1152/ajpcell.00457.2023.

43. Pang, X.-S., Zhang, P., Chen, X.-P., Liu, W.-M. Ubiquitin–Proteasome Pathway in Skeletal Muscle Atrophy. Front. Physiol. 2023;14:1289537. https://doi.org/10.3389/fphys.2023.1289537.

44. Zhong, Q., Zheng, K., Li, W., An, K., Liu, Y., Xiao, X., Hai, S., Dong, B., Li, S., An, Z., Dai, L. Post-Translational Regulation of Muscle Growth, Muscle Aging and Sarcopenia. J. Cachexia Sarcopenia Muscle 2023;14(3):1212–1227. https://doi.org/10.1002/jcsm.13241.

45. Liang, W., Xu, F., Li, L., Peng, C., Sun, H., Qiu, J., Sun, J. Epigenetic Control of Skeletal Muscle Atrophy. Cell. Mol. Biol. Lett. 2024;29(1):99. https://doi.org/10.1186/s11658-024-00618-1.

46. Olie, C.S., O'Brien, D.P., Jones, H.B.L., Liang, Z., Damianou, A., Sur-Erdem, I., Pinto-Fernández, A., Raz, V., Kessler, B.M. Deubiquitinases in Muscle Physiology and Disorders. Biochem. Soc. Trans. 2024;52(3):1085–1098. https://doi.org/10.1042/BST20230562.

47. Souglis, A., Bourdas, D.I., Gioldasis, A., Ispirlidis, I., Philippou, A., Zacharakis, E., Apostolidis, A., Efthymiou, G., Travlos, A.K. Time Course of Performance Indexes, Oxidative Stress, Inflammation, and Muscle Damage Markers after a Female Futsal Match. Sports 2023;11(7):127. https://doi.org/10.3390/sports11070127.

48. Barnig, C., Lutzweiler, G., Giannini, M., Lejay, A., Charles, A.-L., Meyer, A., Geny, B. Resolution of Inflammation after Skeletal Muscle Ischemia–Reperfusion Injury: A Focus on the Lipid Mediators Lipoxins, Resolvins, Protectins and Maresins. Antioxidants 2022;11(6):1213. https://doi.org/10.3390/antiox11061213.

49. Stratos, I., Behrendt, A.-K., Anselm, C., Gonzalez, A., Mittlmeier, T., Vollmar, B. Inhibition of TNF-α Restores Muscle Force, Inhibits Inflammation, and Reduces Apoptosis of Traumatized Skeletal Muscles. Cells 2022;11(15):2397. https://doi.org/10.3390/cells11152397.

50. Tian, X., Gao, Z., Yin, D., Hu, Y., Fang, B., Li, C., Lou, S., Rao, Z., Shi, R. 17β-Estradiol Alleviates Contusion-Induced Skeletal Muscle Injury by Decreasing Oxidative Stress via the SIRT1/PGC-1α/Nrf2 Pathway. Steroids 2023;191:109160. https://doi.org/10.1016/j.steroids.2022.109160.

51. Jackson, M.J., Pollock, N., Staunton, C.A., Jones, S., McArdle, A. Redox Control of Signalling Responses to Contractile Activity and Ageing in Skeletal Muscle. Cells 2022;11(10):1698. https://doi.org/10.3390/cells11101698.

52. Canals-Garzón, C., Guisado-Barrilao, R., Martínez-García, D., Chirosa-Ríos, I.J., Jerez-Mayorga, D., Guisado-Requena, I.M. Effect of Antioxidant Supplementation on Markers of Oxidative Stress and Muscle Damage after Strength Exercise: A Systematic Review. Int. J. Environ. Res. Public Health 2022;19(3):1803. https://doi.org/10.3390/ijerph19031803.

53. Taylor, D.F., Bishop, D.J. Transcription Factor Movement and Exercise-Induced Mitochondrial Biogenesis in Human Skeletal Muscle: Current Knowledge and Future Perspectives. Int. J. Mol. Sci. 2022;23(3):1517. https://doi.org/10.3390/ijms23031517.

54. Kong, S., Cai, B., Nie, Q. PGC-1α Affects Skeletal Muscle and Adipose Tissue Development by Regulating Mitochondrial Biogenesis. Mol. Genet. Genomics 2022;297(3):621–633. https://doi.org/10.1007/s00438-022-01878-2.

55. Gurd, B.J., Menezes, E.S., Arhen, B.B., Islam, H. Impacts of Altered Exercise Volume, Intensity, and Duration on the Activation of AMPK and CaMKII and Increases in PGC-1α mRNA. Semin. Cell Dev. Biol. 2023;143:17–27. https://doi.org/10.1016/j.semcdb.2022.05.016.

56. Smith, J.A.B., Murach, K.A., Dyar, K.A., Zierath, J.R. Exercise Metabolism and Adaptation in Skeletal Muscle. Nat. Rev. Mol. Cell Biol. 2023;24(9):607–632. https://doi.org/10.1038/s41580-023-00606-x.

57. de Araújo, L.T., da Silva, P.C., Masini, M. Medical Ozone as a Therapeutic Option in Musculoskeletal Pain Control: A Critical Review of Clinical Trials Considering Safety and Quality Indicators for Procedures and Devices. Yale J. Biol. Med. 2024;97(3):383–398. https://doi.org/10.59249/HGTG9363.

58. Arias-Vázquez, P.I., Guzzardo, M.N., Guzzardo, D.R., Castillo-Avila, R.G., Tovilla-Zárate, C.A., Montiel, M.A.A. Efficacy of Ozone Injections for Reducing Musculoskeletal Pain in Comparison with Corticosteroid Injections: A Systematic Review and Meta-Analysis. J. Back Musculoskelet. Rehabil. 2024;37(4):821–838. https://doi.org/10.3233/BMR-230173.

59. Hickey, A.J., Maloney, S.E., Kuehl, P.J., Phillips, J.E., Wolff, R.K. Practical Considerations in Dose Extrapolation from Animals to Humans. J. Aerosol Med. Pulm. Drug Deliv. 2024;37(2):77–89. https://doi.org/10.1089/jamp.2023.0041.

60. Spanagel, R. Ten Points to Improve Reproducibility and Translation of Animal Research. Front. Behav. Neurosci. 2022;16:869511. https://doi.org/10.3389/fnbeh.2022.869511.

61. Della Peruta, C., Lozanoska-Ochser, B., Renzini, A., Moresi, V., Sanchez Riera, C., Bouché, M., Coletti, D. Sex Differences in Inflammation and Muscle Wasting in Aging and Disease. Int. J. Mol. Sci. 2023;24(5):4651. https://doi.org/10.3390/ijms24054651.

62. McCartan, A.J.S., Mrsny, R.J. In Vitro Modelling of Intramuscular Injection Site Events. Expert Opin. Drug Deliv. 2024;21(8):1155–1173. https://doi.org/10.1080/17425247.2024.2388841.

Supplementary Files

This is a list of supplementary files associated with this preprint. Click to download.

- SupplementaryFiles.zip
- OringinalimagesforBlot.zip